

# 1     **Formation mechanism of freezing interface strain and the** 2     **effects of different factors on freezing interface strain**

3     Jingfu Jin<sup>a,b</sup>, Yiyi Chen<sup>a</sup>, Tingkun Chen<sup>a,b,\*</sup>, Yingchun Qi<sup>a</sup>, Qian Cong<sup>b</sup>, Chaozong

4                                     Liu<sup>c</sup>

5     <sup>a</sup> College of Biological and Agricultural Engineering, Jilin University, Changchun  
6     130022, P. R. China.

7     <sup>b</sup> Key Laboratory of Bionic Engineering, Ministry of Education, Jilin University,  
8     Changchun 130022, P. R. China.

9     <sup>c</sup> Department of Ortho and MSK Science, University College London, London HA7  
10    4LP, United Kingdom.

## 11    **Abstract**

12       The research studied the freezing interface change during the freezing process to  
13    explain the ice adhesion mechanism. Formation and variation of the freezing interface  
14    strain of different volumes of water on aluminum alloy at different ambient  
15    temperatures were tested. The experimental results showed that the interface strain  
16    had the same formation and variation law regardless of volumes of water and ambient

---

\* Corresponding author at: Jilin University, 5988 Renmin Street, Changchun 130025,  
P. R. China.

E-mail address: [chentk@jlu.edu.cn](mailto:chentk@jlu.edu.cn) (T. Chen); Tel: +86-13194377917; Fax: +86-0431-  
85095253

1 temperatures. The freezing interface strain formation process could be separated into a  
2 decreasing stage, a rapid increase, and a stable stage. The freezing interface strain  
3 gradually increased with the lower ambient temperature or the increase in the volume  
4 of water. Combined with the freezing process, the freezing time of the attached water  
5 and the formation time of swelling force was early with the decrease in ambient  
6 temperature. And ice adhesion area was small, so the freezing interface strain  
7 increased. When the volume of water increased, although the contact area between ice  
8 and substrate increased, the internal energy contained in water increased, which led to  
9 the swelling force increasing, so interface stain increased. The study would help  
10 analyze the formation process of ice adhesion and strength from the mechanical  
11 properties and lay a theoretical foundation for developing process-intervention  
12 anti/de-icing technology.

13 **Keywords:** low temperature; ice adhesion; interface strain; phase change; variable  
14 regularity; formation process

## 15 **1. Introduction**

16 In high latitude or high altitude areas, the water in the environment easily  
17 adheres to the material surface and freezes into ice. Then the adhesion strength is  
18 formed between the accreted ice and the material, which is difficult to remove.  
19 Freezing and ice adhesion are common phenomena, bringing many hazards to  
20 engineering, such as power transmission, aviation, transportation, renewable energy,  
21 and other engineering fields. The surface of power transmission components such as

1 transmission lines and towers in high-latitude or high-altitude areas is prone to  
2 accumulate a large amount of ice, increasing the load, leading to cable breakage,  
3 tower collapse, and damage to the power transmission network (Jin et al., 2022; Wang  
4 2017; Zhuo et al., 2021). For example, the freezing disaster in southern China in 2008  
5 paralyzed the power network, and the direct economic loss was over 150 billion RMB  
6 (Jin et al., 2022; Lv et al., 2014). Once the accumulated ice adhesive on the surfaces  
7 of aircraft wings, sensors, and other components, the aerodynamic performance,  
8 handling, and stability of the aircraft will be affected, and the flight safety of aircraft  
9 will be reduced (Caliskan and Hajiyev 2013; Douglass and Palacios, 2021). In cold  
10 regions, a mixture of ice, snow, and other materials adhered to the chassis component  
11 surfaces of high-speed trains affects the operational safety, service life of components,  
12 and comfort (Cai et al., 2021; Olofsson et al., 2015). With the increasing consumption  
13 of traditional energy, the demand for renewable energy is gradually increasing.  
14 However, ice adhesion affects the development of the new energy industry. Such as,  
15 the accumulated ice on the blade surface changes the morphology of the blade and  
16 affects the stability of the fan operation, resulting in the occurrence of operation  
17 accidents (Sabatier et al., 2016; Manabayev et al., 2021). Meanwhile, the accumulated  
18 ice on the surface of photovoltaic panels reduces photoelectric conversion efficiency  
19 (Jelle 2013; Borrebaek et al., 2020). In addition, ice adhesion also has a severe impact  
20 on refrigeration, offshore platforms, ship transportation, and other industries (Fillion  
21 et al., 2017; Li et al., 2020; Zhang and Lv, 2015). Hence, ice adhesion has seriously

---

*Abbreviations:* RMB, renminbi (also known as CNY, Chinese yuan).

1 impacted the engineering field and people's lives.

2 To reduce the harm of ice adhesion, researchers have developed many kinds of  
3 anti/de-icing technologies. According to the working principle of methods, the  
4 conventional anti-icing methods can be divided into physical and chemical methods,  
5 of which physical methods include mechanical and heating anti/de-icing ways ([Chen  
6 et al., 2019](#); [Guerin et al., 2016](#); [Jin et al., 2022](#); [Rashid et al., 2016](#)). However, the  
7 heating anti/de-icing method is to increase the surface temperature to delay the  
8 freezing time of water or melt the accreted ice at the expense of consuming a lot of  
9 heat ([Mohseni and Amirfazli, 2013](#); [Jin et al., 2018](#)). The chemical anti/de-icing agent  
10 that is not recycled after use can lead to corrosion of parts, water pollution, and soil  
11 compaction ([Gao et al., 2021](#); [Tong et al., 2019](#); [Xia et al., 2020](#)). Hence, the  
12 conventional anti-icing methods have disadvantages during actual use, such as high  
13 energy consumption, high cost, environmental pollution, etc. ([Ringdahl et al., 2021](#)).  
14 With the continuous development of material preparation technology and the  
15 discovery of the lotus leaf effect, researchers have devoted themselves to developing  
16 superhydrophobic surfaces by changing the material surface characteristics, such as  
17 surface energy and wettability. Because the superhydrophobic surface can delay the  
18 freezing time of water on the material surface, reduce the contact area between ice  
19 and substrate, and reduce the surface icing adhesion strength, the superhydrophobic  
20 surface is considered as one of the potential anti/de-icing methods ([Jin et al., 2022](#);  
21 [Rashid et al., 2016](#); [Zhang and Lv, 2015](#)). However, the present study has shown the  
22 drawbacks of superhydrophobic surfaces in the lab environment, such as poor anti/de-

1 icing durability and mechanical stability (Chen et al., 2012; Jain and Pitchumani,  
2 2018; Mahadik et al., 2013; Oberli et al., 2014; Ozbay and Erbil, 2016; Villegas et al.,  
3 2019; Wang et al., 2012; Wang et al., 2014; Zheng et al., 2016). The wettability of the  
4 superhydrophobic surface was gradually lost, and the micro/nano-structure was  
5 damaged after experiencing multiple freeze-thaw cycles (Mobarakeh et al., 2013;  
6 Zheng et al., 2016; Zheng et al., 2017). And the ice adhesion strength of the  
7 superhydrophobic surface would increase (Mobarakeh et al., 2013). Meanwhile,  
8 simplifying the preparation process of the superhydrophobic surface and reducing the  
9 preparation cost is also one of the challenges of applying the superhydrophobic  
10 surface (Wang et al., 2012; Zheng et al., 2016).

11 To optimize and develop new anti/de-icing methods, the droplets frozen into ice  
12 on a cold surface have been observed using commercial or self-made devices to  
13 provide theoretical support. The previous study has shown that the freezing process  
14 can be divided into multi-stages: water spreading on the material surface, the  
15 supercooled state after the freezing front appeared, the phase transition, and  
16 completely freezing into the ice with the change of shape (Chen et al., 2018; Cong et  
17 al., 2021; Jin et al., 2014; McDonald et al., 2017). For example, Chen et al. (2019)  
18 proposed an anti-icing method based on phase and volume expansion during the  
19 freezing process based on observing the freezing process. And the surface wettability  
20 is changed to reduce the amount of water attached to the material surface. According  
21 to the formation conditions and freezing process of ice, the experiment on the  
22 influence of factors on the ice adhesion strength has also been carried out to optimize

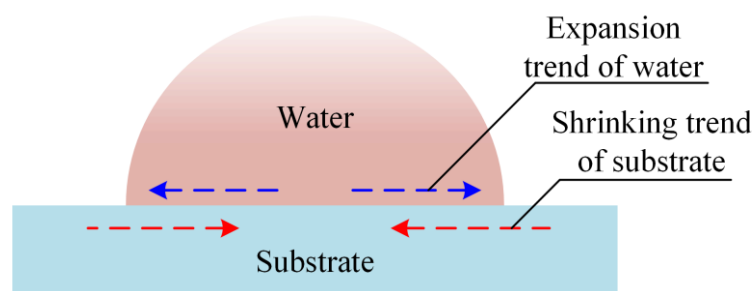
1 the conventional anti/de-icing technology. The factors include wettability, ambient  
2 temperature, the initial temperature of the material surface, freezing time, surface  
3 roughness, etc. (Chen et al., 2018; Emelyanenko et al., 2020; Memon et al., 2020;  
4 [Fillion et al., 2017](#); [Yan et al., 2014](#); [Work and Lian, 2018](#);) Such as, the surface  
5 temperature is increased by heating to delay freezing time or remove the accreted ice  
6 on the material surface. This is also the main direction in the current anti/de-icing  
7 research. However, little research has been done on the ice-solid adhesion interface  
8 strain or stress change during the freezing process.

9 Due to the difference in the expansion coefficient between water/ice and the  
10 matrix, interfacial stress will be generated when the water phases into ice on the  
11 material surface during the freezing process. The present study aims to collect the  
12 strain of the adhesion interface between water/ice and substrate during the freezing  
13 process of different volumes of water in different low-temperature environments, and  
14 analyze the formation process and variation regularity of the interface strain/stress. It  
15 is beneficial to understand the formation mechanism of the ice adhesion strength and  
16 determine the relationship between the adhesion interface stress and the adhesion  
17 strength by studying the interface strain/stress formation during the freezing process.  
18 Furthermore, it will provide a reference for developing a new active anti/de-icing  
19 technology by affecting or changing the adhesive interface stress to reduce the ice  
20 adhesion strength.

## 21 **2. Materials and methods**

22 It is well known that water expands in volume during freezing, and other

1 materials do not expand in a low-temperature environment. Because different  
2 materials have different expansion coefficients, the expansion directions of water/ice  
3 and the substrate during the freezing process are shown in Fig. 1. Hence, the water  
4 attached to the material surface expands outward along the interface direction during  
5 the freezing process, and the substrate can shrink in a low-temperature environment.  
6 Water/ice and substrate deform in different directions at low temperatures.

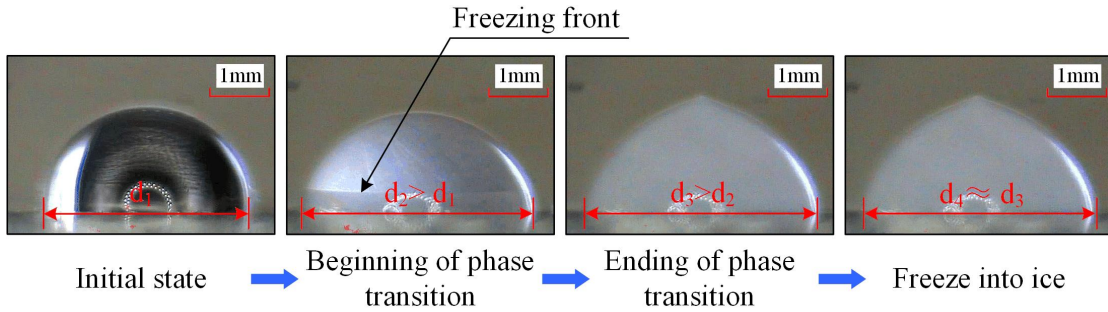


7

8 Fig. 1. The direction of deformation of water and substrate during freezing.

9 Hence, the contact diameter between water/ice and the substrate during the  
10 freezing process was observed using a purpose-built device. The experimental  
11 procedure and the apparatus were reported in detail in a previous study (Chen et al.,  
12 2018). The contact diameter between water/ice and the material surface at different  
13 stages during the freezing process was calculated by using the tracepoint method  
14 (Cong et al., 2021; Chaudhary and Li, 2014; Fumoto and Kawanami, 2012; Hui and  
15 Jin, 2010; Lazauskas et al., 2013; Xu et al., 2012), as shown in Fig. 2. It could be seen  
16 that the contact diameter between the mixture formed by water and ice and the  
17 substrate after the phase transition was larger than the contact diameter between the  
18 water and the substrate in the initial state. After water solidified into ice, the contact  
19 diameter tent to be stable. The phase transition process was the main stage of the

1 interfacial contact diameter change during the freezing process. So, strain gauges  
2 were used to measure the strain of the adhesion interface during the freezing process.



4 Fig. 2. Changes in the diameter of the contact interface before and after the freezing  
5 process.

## 6 2.1 Materials

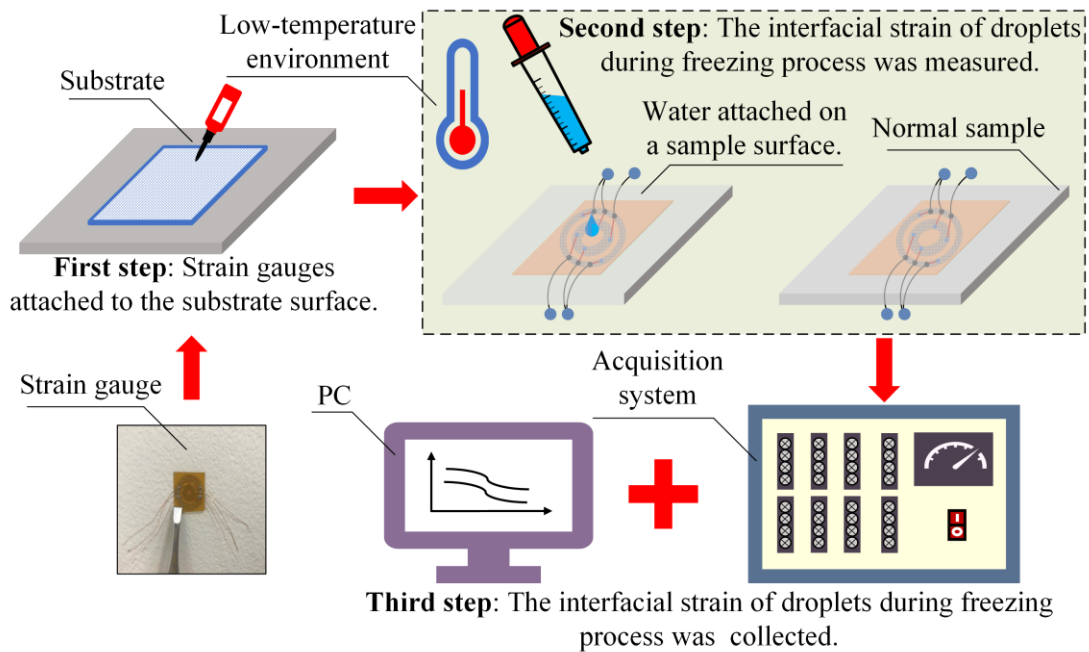
7 During the present study, 1060 aluminum alloy was purchased from the Haerbin  
8 Dongbeilong Metal Co., Ltd., as the sample material. Pure water and acetone (Tianjin  
9 East China Chemicals Co. Ltd.) were used for ice preparation and material cleaning.  
10 In the experiment, a circular strain gauge (model size: BHF350-12KA) purchased  
11 from Taizhou Huangyan Electronic Components Co., Ltd., was used to measure the  
12 interface strain during the freezing process. The 502-cyanoacrylate adhesive  
13 (Zhejiang Jiuerjiu Chemicals Co., Ltd.) was used to contact the strain gauge and the  
14 substrate, and 703-one component room temperature vulcanized silicon rubber  
15 completely covered the strain gauge.

## 16 2.2 Experimental device

17 A test device was designed to measure and collect the interface strain during the  
18 freezing process, as shown in Fig. 3. The device was composed of a climate chamber



1 controlling the ambient temperature, a strain acquisition system, and other  
 2 components. During the freezing process, the freezing interface strain was collected in  
 3 real-time by adopting the strain acquisition system purchased from Nanjing Danmo  
 4 Electronic Technology Co., Ltd., model DM-YB1808. The acquisition frequency of  
 5 the system is 20 Hz, and the temperature control accuracy of the climate chamber is  
 6  $\pm 0.01$  °C. Meanwhile, the ambient temperature around the sample was collected  
 7 synchronously.



8

9 Fig. 3. Interface strain acquisition system during the freezing process.

10 The samples were cleaned in an acetone ultrasonic bath for 5 minutes and in a  
 11 deionized water ultrasonic bath for another 5 minutes. 502 cyanoacrylate adhesive  
 12 was used to paste the circular strain gauge in the center of the bottom of the sample,  
 13 and the circular strain gauge was covered with silicone rubber. If the resistance of the  
 14 strain gauge before and after pasting was similar, the pasted strain gauge could still  
 15 work normally. After sticking, there should be no air bubbles between the strain gauge

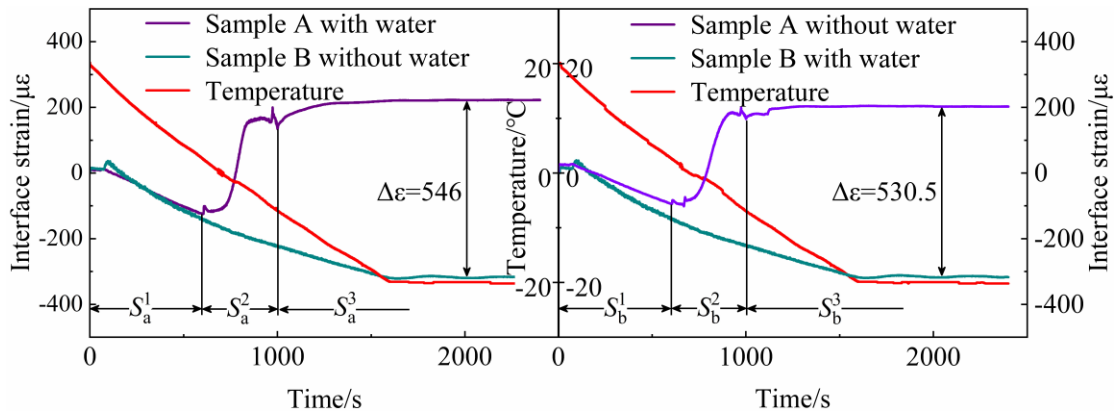
1 and the substrate and the area covered by the silicone rubber.

## 2 2.3 Test methods and details

3 1060 aluminum alloy ( $60 \times 60 \times 0.2 \text{ mm}^3$  in size) was fixed. As shown in [Fig. 3](#),  
4 water was titrated on the central area of the aluminum alloy surface without the strain  
5 gauge attached by a pipette. The climate chamber was set to the target temperature.  
6 The interface strain and the ambient temperature around the sample were collected  
7 synchronously through the collection system. The pairing comparison was used to  
8 calculate the interface strain during the freezing process of different water volumes at  
9 different ambient temperatures. One of the sample surfaces was titrated with water  
10 droplets, while the other was free of water. That was, the sample surface was titrated  
11 with water droplets, and the other sample surface was free of water. The strain  
12 difference between the sample with water on the surface and the sample without water  
13 on the surface was the interfacial strain produced by the freezing process of the  
14 volume of water at the temperature. When the collected strain tended to be stable, the  
15 acquisition system was turned off. The climate chamber was set to the target  
16 temperature.

17 As shown in [Fig. 3](#), in a low-temperature environment, the same volume of water  
18 was titrated successively on the surfaces of different samples to exclude the effects of  
19 the experimental device, various samples, and preparation processes on the  
20 experimental results. An initial test with an ambient temperature of  $-20 \text{ }^\circ\text{C}$  and a water  
21 volume of 2 ml was carried out. Water was titrated on sample A surface during a test  
22 (a), and water was titrated on sample B surface in test (b). And there was no water on

1 other sample surfaces. Fig. 4 showed the interfacial strain of water on different  
 2 sample surfaces during the freezing process.



3  
 4 Fig. 4. Variation of interfacial strain on different sample surfaces during the freezing  
 5 process.

6 It could be seen that the interfacial strain generated by the same volume of water  
 7 on the surface of different samples during freezing had the same variation process.  
 8 The process of the interface strain could be divided into a gradual decrease of the  
 9 interface strain  $S^1$ , a sudden increase  $S^2$ , and a stable stage  $S^3$ . The interfacial strain  
 10 produced by the freezing process was similar in test (a) and test (b), and the difference  
 11 in interfacial strain in the two tests was less than 5%. Therefore, the interface strain  
 12 produced by the freezing process could be measured and collected using the  
 13 experimental device. During the test, the volume of water on the sample surface was  
 14 0.5 ml, 1.0 ml, 1.5 ml, and 2.0 ml, respectively. And the ambient temperature was -  
 15 5 °C, -10 °C, -15 °C, and -20 °C, respectively.

### 16 3. Results

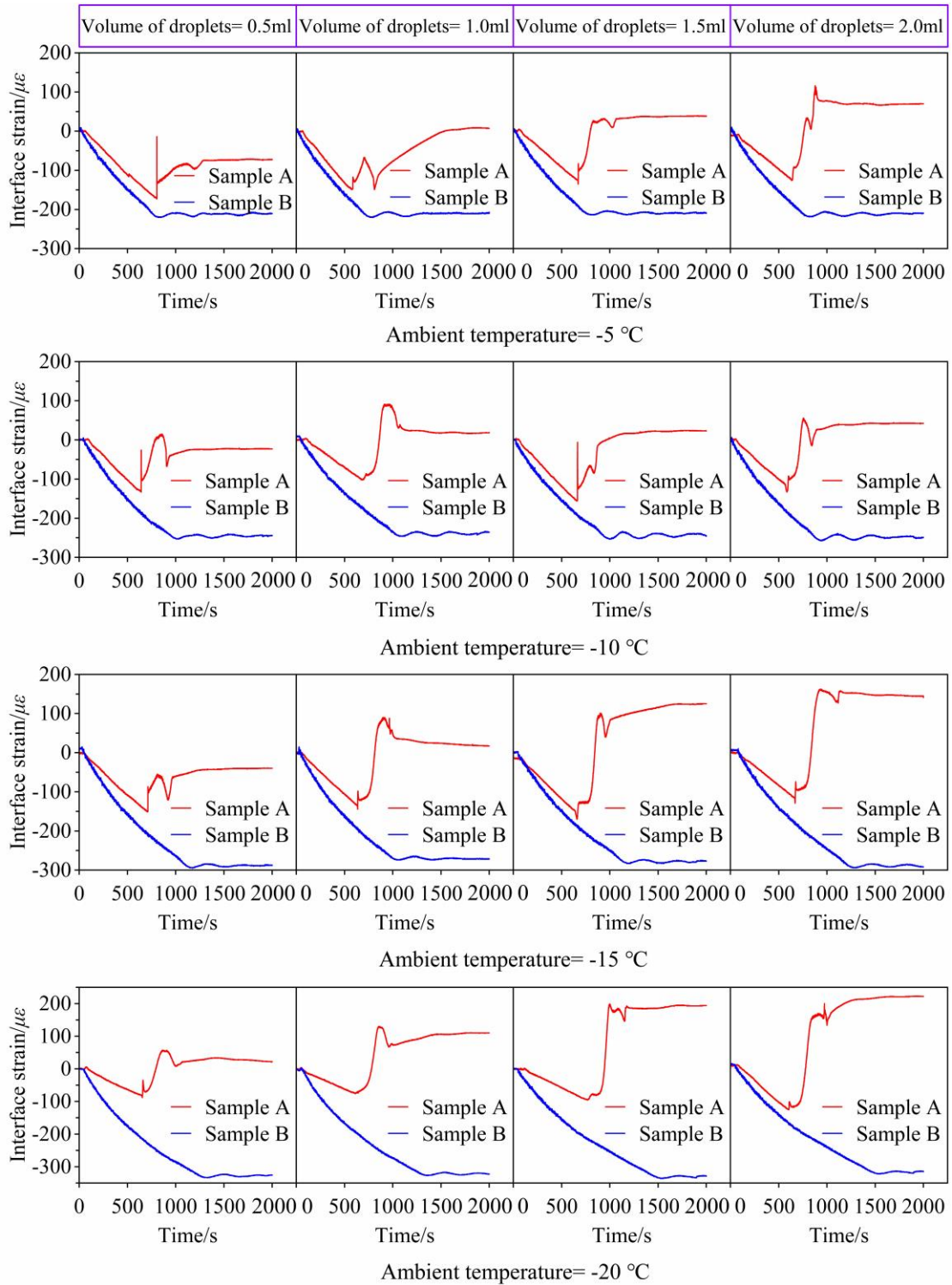
#### 17 3.1 Freezing interface strain

1       The samples with and without water on the surface of the sample were named  
2 samples A and B, respectively. The adhesion interface strain during the freezing  
3 process of different volumes of water measured and collected at different ambient  
4 temperatures was shown in [Fig. 5](#).

5       The changes in the adhesion interface strain during the freezing process of  
6 different volumes of water at different temperatures were similar, which was also  
7 similar to the change of the interface strain in the initial verification test (as shown in  
8 [Fig. 4](#)). Therefore, the adhesion interface strain change during the freezing process  
9 could be divided into a stage where the interface strain gradually decreases and tends  
10 to be stable after the interface strain increases abruptly. The interfacial strain would  
11 increase abruptly during the variation process of the interfacial strain, whether it was a  
12 large volume of water or a lower ambient temperature. Meanwhile, the adhesion  
13 interface strain would fluctuate with different variation processes in the sudden  
14 increase stage of strain.

15       As the ambient temperature decreased, the interfacial strain of sample B  
16 gradually increased. Since sample B was an aluminum alloy, the strain direction was  
17 inward shrinkage. During the interface strain reduction stage, the formation rate of the  
18 interface strain of sample B was significantly greater than that of sample A.  
19 Meanwhile, the various directions of sample A and sample B interfacial strains were  
20 the same. With the increase in the volume of water attached to the sample A surface or  
21 the decrease of the ambient temperature, the interfacial strain generated by the water  
22 on the material surface gradually increases during the freezing process, as shown in

1 Fig. 5.



2

3 Fig. 5. Effects of different water volumes and ambient temperatures on the interface  
4 strain.

5 As the cooling time continued, the difference in the measured interfacial strain

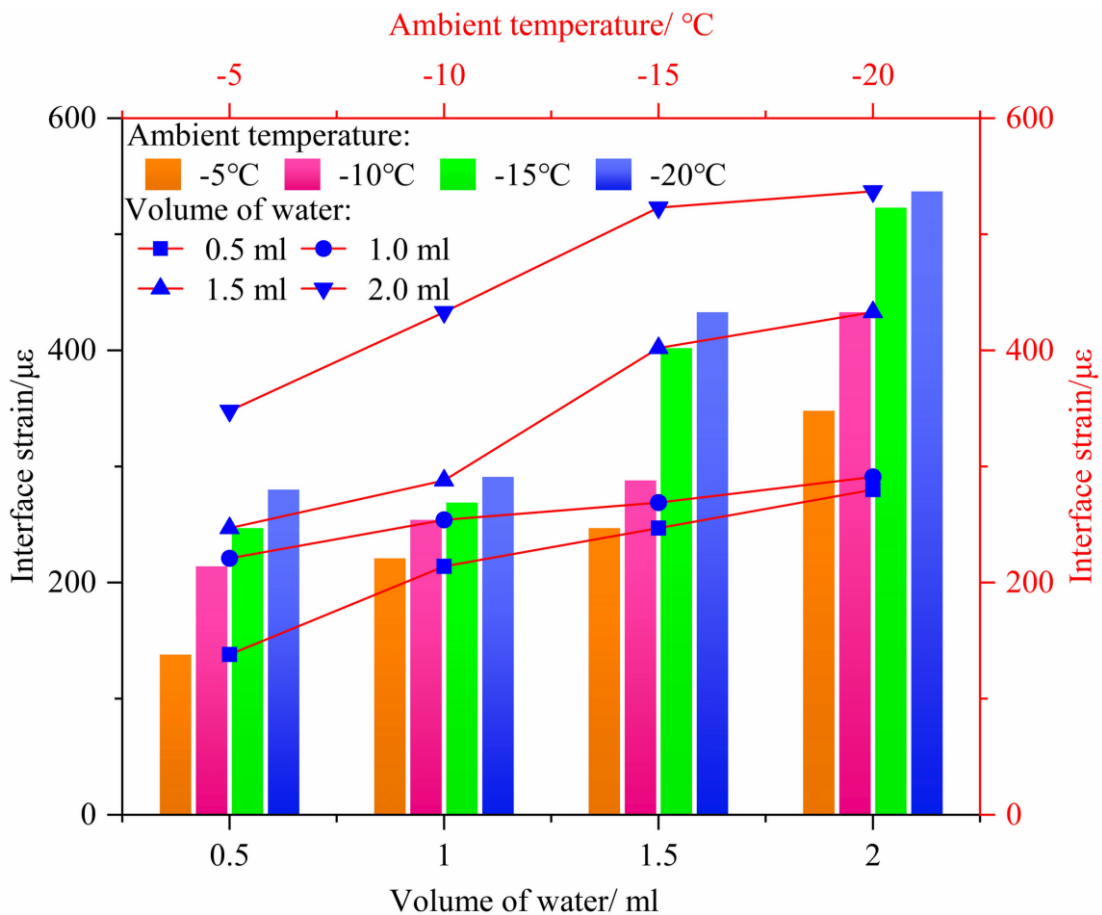
1 between samples A and B in the test gradually increased. Then the strain of the sample  
2 in the test increased suddenly, and the strain variation direction of the sample changed  
3 suddenly. Sample A and sample B had different interfacial strain change directions.  
4 When the ambient temperature was  $-5\text{ }^{\circ}\text{C}$  and  $-10\text{ }^{\circ}\text{C}$ , the interface strain of  
5 aluminum alloy without water on the surface could reach stability first than that of  
6 aluminum alloy with water on the surface. With the decrease of the ambient  
7 temperature, the interfacial strain of sample A with water on the surface could reach  
8 the stable stage first than that of sample B without water on the surface. This could be  
9 seen in [Fig. 5](#).

### 10 3.2 Variation law of the freezing interface strain

11 According to the experimental results, the interfacial strain of water during the  
12 freezing process was calculated relative to the sample strain without water on the  
13 surface collected in each test. In different low-temperature environments, the  
14 interfacial strains generated by different volumes of water during the freezing process  
15 were shown in [Fig. 6](#).

16 With the decrease of the ambient temperature and the increase volume of the  
17 attached water, the adhesion interface strain gradually increased during the freezing  
18 process. When the ambient temperature was constant, the adhesive interface strain  
19 increased with an increased volume of water attached to the surface, as shown in [Fig.](#)  
20 [6](#). As the same volume of water was attached to the sample A surface, the adhesive  
21 interface strain increased gradually with the decrease of the ambient temperature  
22 during the freezing process. When different volumes of water were attached to the

1 aluminum alloy surface during the experiment, the adhesive interface strain gradually  
 2 tended to be stable during the freezing process as the ambient temperature decreased.  
 3 With the decrease in the ambient temperature, the interfacial strain gradually tended to  
 4 be the same during the freezing process of 0.5 ml and 1.0 ml of water on the material  
 5 surface. When the volume of water attached to the material surface was 2.0 ml, the  
 6 interfacial strain increased approximately in a linear trend. When the ambient  
 7 temperature was -20 °C, the increment of growth in the interface strain decreased  
 8 relative to the ambient temperature of -15 °C. It could be seen from the line graph in  
 9 Fig. 6.



10

11 Fig. 6. Variation of interface strain under different experimental conditions.

12

When the ambient temperature was -5 °C and -10 °C, compared with other

1 volumes of water attached to the aluminum alloy surface, the interfacial strain  
2 produced by 2.0ml of water during the freezing process of the aluminum alloy surface  
3 suddenly increased. Meanwhile, when the ambient temperature was -15 °C and -20 °C,  
4 respectively, the interfacial strain produced by 1.5 ml and 2.0 ml of water during the  
5 freezing process on the aluminum alloy surface was significantly greater than that  
6 produced by 0.5 ml and 1.0 ml of water during the freezing process.

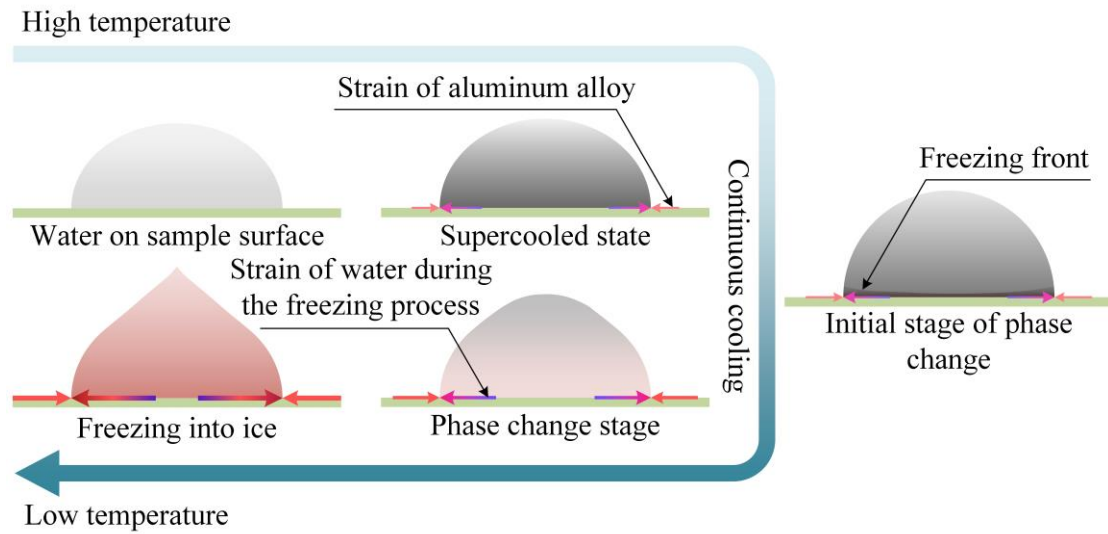
## 7 **4. Discussion**

### 8 4.1 Formation mechanism of the freezing interface strain

9 The freezing process of water on the material surface and the change of the  
10 freezing interface strain are shown in Fig. 7. The aluminum alloy shrank inward under  
11 the low-temperature environment, and the strain  $\varepsilon_1$  of the sample gradually increased  
12 until the ambient temperature did not change. When the ambient temperature  
13 decreased to the target temperature, the attached water on the aluminum alloy surface  
14 gradually entered the supercooled state. The contact diameter between the water and  
15 the material surface would increase during the freezing process, as shown in Fig. 2.  
16 The direction of the strain  $\varepsilon_2$  generated by the water in the supercooled state was  
17 outward along with the freezing interface, opposite to the strain  $\varepsilon_1$  of the aluminum  
18 alloy sample shrinking at the low temperature. It could be seen from the supercooled  
19 stage in Fig. 7. Compared with the strain reduction rate of the aluminum alloy without  
20 attaching water in the  $S^1$  stage, this would reduce the strain reduction rate of  
21 aluminum alloy with water on the surface. It was similar to the experimental results



1 shown in Fig. 5.



2

3 Fig. 7. The freezing process of water attached to aluminum alloy surface and the  
4 change of interfacial strain.

5 At the initial stage of phase transformation, a freezing front appeared inside the  
6 attached water, and the attached water near the surface of the material began to freeze  
7 after the freezing front moved (as shown in the initial stage of phase change in Fig. 7).

8 During the phase transformation process of the attached water, the strain  $\varepsilon_2$  of the  
9 freezing interface was gradually larger than the shrinkage strain  $\varepsilon_1$  of the aluminum  
10 alloy in the low-temperature environment, which gradually changed the strain  
11 direction of the aluminum alloy sample with water. Meanwhile, the edge of water  
12 attached to the aluminum alloy surface was frozen first, limiting the expansion of the  
13 attached water along the tangential direction of the interface during the freezing  
14 process. The aluminum alloy sample had a limiting effect on the formation of the  
15 adhesion medium. That was, the adhesion strength between the ice and the substrate  
16 was formed. The volume of water could increase abruptly and exert an expansion

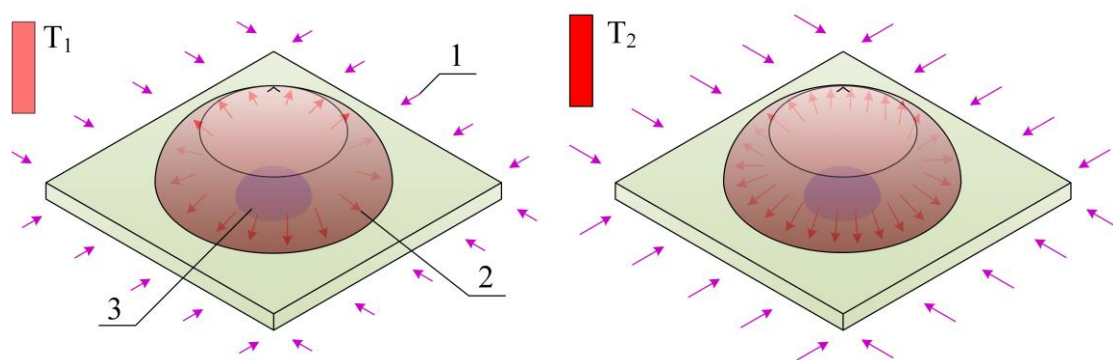
1 force on the boundary constraints as the freezing process continued. The freezing  
2 interface strain would suddenly increase. It could be seen from the stage of complete  
3 freezing into ice in Fig. 7. It was the  $S^2$  stage in Fig. 4. With the increase of phase  
4 transformation expansion stress in the tangential direction during the freezing process,  
5 the tangential ice adhesion strength between accreted ice and aluminum alloy also  
6 increased.

7         Since the cold surface formed a constraining boundary for the attached water, the  
8 freezing interface could not change significantly after the water attached to the  
9 aluminum alloy surface froze into ice, as shown in Fig. 4. When the test environment  
10 reached the predetermined temperature, the aluminum alloy strain gradually stabilized.  
11 Compared with the strain direction of the aluminum alloy without the attached water,  
12 the aluminum alloy surface with adhering water had the opposite strain direction. This  
13 could be seen from the experimental result shown in Fig. 5.

#### 14 4.2 Influence mechanism of different factors on the freezing interface strain

15         Fig. 8 showed the effect of the test temperature on the freezing interface strain  
16 during the freezing process. The test temperature  $T_1$  was higher than that of  $T_2$ . When  
17 the experiment temperature was high, the internal molecular energy of the water  
18 attached to the material surface was higher than that of water attached to the material  
19 surface in the low-temperature environment, and the time of water in a supercooled  
20 state was longer than that of water in a low-temperature environment. This would  
21 result in the phase transition time of water in the environment with a temperature of  
22  $T_2$  was lower than that of water in the environment with a temperature of  $T_1$ . The

1 contact area between the attached water and the aluminum alloy surface at lower  
 2 ambient temperature  $T_2$  was smaller than that between the attached water and the  
 3 aluminum alloy surface at higher ambient temperature  $T_1$ . It could enlarge the  
 4 influence of the swelling force generated by the freezing process of the attached water  
 5 on the freezing interface strain at lower ambient temperature  $T_2$ . The strain during the  
 6 freezing process was increased. Hence, the freezing interface strain of the same  
 7 volume of attached water on the aluminum alloy surface gradually increased as the  
 8 experiment temperature decreased during the freezing process. It was consistent with  
 9 the test results shown in Fig. 5 and Fig. 6.



Ambient temperature  $T_1$  was lower than ambient temperature  $T_2$ .

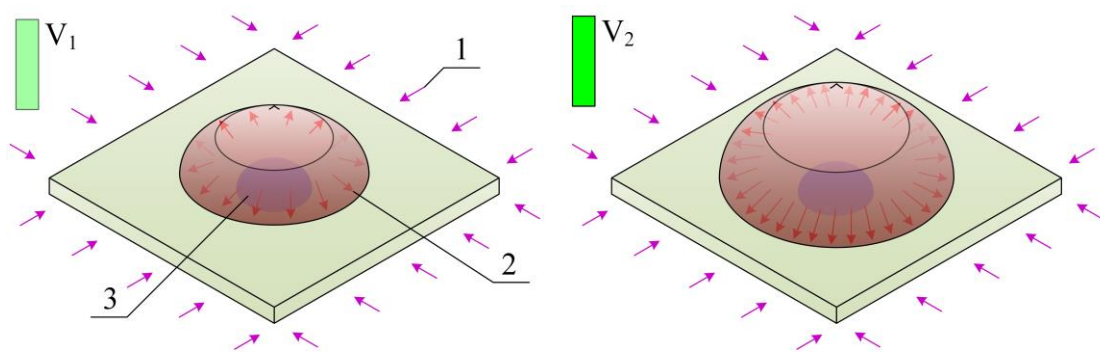
10

11 Fig. 8. Effect of ambient temperature on the freezing interface strain. 1. strain of  
 12 aluminum alloy in a low-temperature environment; 2. strain at the freezing interface  
 13 during the freezing process; 3. strain sensor at the bottom of aluminum alloy.

14 Fig. 9 showed the effect of the volume of water on the freezing interface strain.  
 15 In a low-temperature environment, the phase transformation process of a small  
 16 volume of water could last for a short time. The volume  $V_1$  of water attached to the  
 17 substrate surface was smaller than that of  $V_2$ . Hence, the contact area between

1 water/ice and the aluminum alloy was different.

2 The interfacial strain was generated when the water could expand outward  
3 during the freezing process. With the increase in the volume of water attached to the  
4 material surface, the internal energy stored in the water was increased, and the  
5 expansion force released by the water in the phase change process was increased.  
6 Because the substrate with low temperature would form a fixed constraint on the  
7 attached ice, the tendency of water to expand outward along with the interface during  
8 the freezing process was limited. This would also increase the tendency of water to  
9 expand along the interface direction during the freezing process, and the frozen  
10 interface strain was increased. Therefore, the interfacial strain formed by the smaller  
11 volume of water would be larger than that formed by the larger volume of water  
12 during the freezing process. However, the contact area between water or ice and  
13 aluminum alloy increased with the volume of attached water, and the freezing time  
14 was delayed.



15 The volume  $V_1$  of the attached water was smaller than the volume  $V_2$  of the attached  
16 water.

17 Fig. 9. Effect of water volumes on the freezing interface strain. 1. strain of aluminum  
18 alloy in a low-temperature environment; 2. strain at the freezing interface during the  
freezing process; 3. strain sensor at the bottom of aluminum alloy.

1 Compared with the interfacial strain of the small volume water during phase  
2 transformation, it would reduce the increased rate of interfacial strain of large volume  
3 attached water during the freezing process. This was consistent with the experimental  
4 results.

## 5 **5. Conclusions**

6 In the present study, the formation and variation of the freezing interface strain  
7 during the freezing process of the adhering water of different volumes on the  
8 aluminum alloy surface were measured at different temperatures. Based on the  
9 experimental results and the freezing process, the formation process of the freezing  
10 interface strain during the freezing process of water attached to the aluminum alloy  
11 surface could be divided into three stages. As the ambient temperature was reduced  
12 from room temperature to below 0 °C, the freezing interface strain first decreased, and  
13 the interface strain tended to stabilize after the sudden increase of the interface strain.  
14 In the experiment, the freezing interface strain could be summarized into these three  
15 stages during the freezing process of different volumes of water in different  
16 temperature environments. When the volume of water attached to the aluminum alloy  
17 surface was the same, the freezing interface strain increased with the decrease of the  
18 ambient temperature during the freezing process. As the ambient temperature was the  
19 same, the freezing interface strain increased with the increase of the volume of water  
20 attached to the aluminum alloy surface during the freezing process. For example,  
21 when the ambient temperature was -5 °C, the order of the freezing interface strains  
22 generated by the freezing process of four different volumes of water was 2.0 ml, 1.5

1 ml, 1.0 ml, and 0.5 ml. In four different ambient temperatures of water with a volume  
2 of 2.0 ml, the order of the freezing interface strains generated by the freezing process  
3 was -20 °C, -15 °C, -10 °C, and -5 °C.

4 It is well known that there is a proportional relationship between strain and stress.  
5 The present study would be helpful for explaining the mechanism of the ice adhesion  
6 process based on the change of the freezing interface strain, and constructing the  
7 relationship between the icing adhesion strength and the interface stress. It is  
8 considered that the formation process of tangential ice adhesion strength is similar to  
9 that of the freezing interface stress. The study could lay a theoretical foundation for  
10 developing new anti/de-icing methods and optimizing existing conventional anti/de-  
11 icing methods, such as process-intervention anti-icing technology. This is the ultimate  
12 research goal of the author's research team.

### 13 **Declaration of Competing Interest**

14 The authors declare that they have no known competing financial interests or  
15 personal relationships that could have influenced the work reported in this paper.

### 16 **Acknowledgements**

17 This work was supported by the Department of Science and Technology of Jilin  
18 Province, China (Grant No. 20220101215JC and 20200801049GH), the Education  
19 Department of Jilin Province, China (Grant No. JJKH20211070KJ).

### 20 **References**

21 Borrebaek, P. O. A., Jelle, B. P., Zhang, Z. L., 2020. Avoiding snow and ice accretion

1 on building integrated photovoltaics-challenges, strategies, and opportunities. Sol.  
2 Energy Mater. Sol. Cells. 206, ID 110306.  
3 <https://doi.org/10.1016/j.solmat.2019.110306>.

4 Chen, J., Liu, J., He, M., et al., 2012. Superhydrophobic surface cannot reduce ice  
5 adhesion. Appl. Phys. Lett. 101(11), ID 111603.  
6 <https://doi.org/10.1063/1.4752436>.

7 Caliskan, F., Hajiyev, C., 2013. A review of in-flight detection and identification of  
8 aircraft icing and reconfigurable control. Prog. Aeosp. Sci. 60, 12-34.  
9 <https://doi.org/10.1016/j.paerosci.2012.11.001>.

10 Chaudhary, G., Li, R., 2014. Freezing of water droplets on solid surfaces an  
11 experimental and numerical study. Exp. Therm. Fluid. Sci. 57, 86-93.  
12 <https://doi.org/10.1016/j.expthermflusci.2014.04.007>.

13 Chen, T. K., Cong, Q., Sun, C. B., et al., 2018. Influence of substrate initial  
14 temperature on adhesion strength of ice on aluminum alloy. Cold Reg. Sci.  
15 Technol. 148, 142-147. <https://doi.org/10.1016/j.coldregions.2018.01.017>.

16 Chen, T. K., Jin, J. F., Qi, Y. C., et al., 2019. Disturbing stability of interface by  
17 adopting phase-change temperature gradient to reduce ice adhesion strength.  
18 Cold Reg. Sci. Technol. 158, 69-75.  
19 <https://doi.org/10.1016/j.coldregions.2018.11.010>.

20 Cai, L., Lou, Z., Li, T., et al., 2021. Numerical study on the effects of anti-snow  
21 deflector on the wind-snow flow underneath a high-speed train. J. Appl. Fluid  
22 Mech. 14(1), 287-299. <https://doi.org/10.47176/JAFM.14.01.31375>.

1 Cong, Q., Xu, J., Ren, L. Q., et al., 2021. Changes of water/ice morphological,  
2 thermodynamic, and mechanical parameters during the freezing process. Arab. J.  
3 Sci. Eng. 46(11), 10631-10639. <https://doi.org/10.1007/s13369-021-05502-0>.

4 Douglass, R. G., Palacios, J. L., 2021. Effects of strain rate variation on the shear  
5 adhesion strength of impact ice. Cold Reg. Sci. Technol. 181, ID 103168.  
6 <https://doi.org/10.1016/j.coldregions.2020.103168>.

7 Emelyanenko, K. A., Emelyanenko, A. M., Boinovich, L. B., 2020. Water and ice  
8 adhesion to solid surfaces: common and specific, the impact of temperature and  
9 surface wettability. Coatings. 10(7), ID 648.  
10 <https://doi.org/10.3390/coatings10070648>.

11 Fumoto, K., Kawanami, T., 2012. Study on freezing characteristics of supercooled  
12 water droplets impacting on solid surface. J. Adhes. Sci. Technol. 26(4–5), 463-  
13 472. <https://doi.org/10.1163/016942411X574600>.

14 Fillion, R. M., Riahi, A. R., Edrisy, A., 2017. Design factors for reducing ice adhesion.  
15 J. Adhes. Sci. Technol. 31(21), 2271-2284.  
16 <https://doi.org/10.1080/01694243.2017.1297588>.

17 Guerin, F., Laforte, C., Farinas, M. I., et al., 2016. Analytical model based on  
18 experimental data of centrifuge ice adhesion tests with different substrates. Cold  
19 Reg. Sci. Tech. 121, 93-99. <https://doi.org/10.1016/j.coldregions.2015.10.011>.

20 Gao, H. T., Jian, Y. M., Yan, Y. Y., 2021. The effects of bio-inspired micro/nano scale  
21 structures on anti-icing properties. Soft Matter. 17(3), 447-466.  
22 <https://doi.org/10.1039/D0SM01683G>.



- 1 Hui, H., Jin, Z. Y., 2010. An icing physics study by using lifetime-based molecular  
2 tagging thermometry technique. *Int. J. Multiph. Flow.* 36(8), 672-681.  
3 <https://doi.org/10.1016/j.ijmultiphaseflow.2010.04.001>.
- 4 Jelle, B. P., 2013. A review of the recent advances in superhydrophobic surfaces and  
5 the emerging energy-related applications. *Energy Build.* 67, 334-351.  
6 <https://doi.org/10.1016/j.energy.2015.01.061>.
- 7 Jin, Z. Y., Wang, Y. M., Yang, Z. G., 2014. An experimental investigation into the  
8 effect of synthetic jet on the icing process of a water droplet on a cold surface.  
9 *Int. J. Heat Mass Transf.* 72, 553-558.,  
10 <https://doi.org/10.1016/j.ijheatmasstransfer.2014.01.041>.
- 11 Jin, Z. Y., Chen, M. M., Yang, Z. G., 2018. An experimental investigation of the  
12 melting process of an ice bead in a hot shear flow. *Int. J. Heat Mass Transf.* 125,  
13 190-201. <https://doi.org/10.1016/j.ijheatmasstransfer.2018.04.061>.
- 14 Jain, R., Pitchumani, R., 2018. Facile fabrication of durable copper-based  
15 superhydrophobic surfaces via electrodeposition. *Langmuir.* 34(10), 3159-3169.  
16 <https://doi.org/10.1021/acs.langmuir.7b02227>.
- 17 Jin, J. F., Chen, Y. Y., Qi, Y. C., et al., 2022. Changes in the interfacial stress of water  
18 on aluminum alloy surface during the freezing and thawing process. *Cold Reg.*  
19 *Sci. Tech.* 194, ID 103460. <https://doi.org/10.1016/j.coldregions.2021.103460>.
- 20 Lazauskas, A., Guobience, A., Prosyčevs, I., et al., 2013. Water droplet behavior on  
21 superhydrophobic SiO<sub>2</sub> nanocomposite films during icing/deicing cycles. *Mater.*  
22 *Charact.* 82, 9-16. <https://doi.org/10.1016/j.matchar.2013.04.017>.

- 1 Lv, J. Y., Song, Y. L., Jiang, L., et al., 2014. Wang, Bio-inspired strategies for anti-  
2 icing. ACS Nano. 8 (4), 3152-3169. <https://doi.org/10.1021/nn406522n>.
- 3 Li, T., Lbanez-Ibanze, P. F., Hakonsen, V., et al., 2020. Self-deicing electrolyte  
4 hydrogel surfaces with pa-level ice adhesion and durable antifreezing/antifrost  
5 performance. ACS Appl. Mater. Interfaces. 12(31), 35572-35578.  
6 <https://doi.org/10.1021/acsami.0c06912>.
- 7 Mohseni, M., Amirfazli, A., 2013. A novel electro-thermal anti-icing system for fiber-  
8 reinforced polymer composite airfoils. Cold Reg. Sci. Tech. 87, 47-58.  
9 <https://doi.org/10.1016/j.coldregions.2012.12.003>.
- 10 Mahadik, S. A., Fernando, P. D., Hegade, N. D., et al., 2013. Durability and restoring  
11 of superhydrophobic properties in silica-based coatings. J. Colloid Interface Sci.  
12 405, 262-268. <https://doi.org/10.1016/j.jcis.2013.04.042>.
- 13 Mobarakeh, L. F., Jafari, R., Farzaneh, M., et al., 2013. The ice repellency of plasma  
14 polymerized hexamethyldisiloxane coating. Appl. Surf. Sci. 284, 459-463.  
15 <https://doi.org/10.1016/j.apsusc.2013.07.119>.
- 16 McDonald, B., Patel, P., Zhao, B. X., et al., 2017. Droplet freezing and ice adhesion  
17 strength measurement on super-cooled hydrophobic surfaces. J. Adhes. 93(5),  
18 375-388., <https://doi.org/10.1080/00218464.2015.1077329>.
- 19 Memon, H., Liu, J. P., De Focatiis, D S. A. X., et al., 2020. Intrinsic dependence of ice  
20 adhesion strength on surface roughness. Surf. Coat. Technol. 358, ID 125382.  
21 <https://doi.org/10.1016/j.surfcoat.2020.125382>.
- 22 Manabayev, R., Baizhuma, Z., Bolegenova, S., et al., 2021. Numerical simulations on

1 static vertical axis wind turbine blade icing. *Renew. Energy.* 170, 997-1007.  
2 <https://doi.org/10.1016/j.renene.2021.02.023>.

3 Nosonovsky, M., Hejazi, V., 2012. Why superhydrophobic surfaces are not always  
4 icephobic. *ACS Nano.* 6(10), 8488-8491. <https://doi.org/10.1021/nn302138r>.

5 Oberli, L., Caruso, D., Hall, C., et al., 2014. Condensation and freezing of droplets on  
6 superhydrophobic surfaces. *Adv. Colloid Interf. Sci.* 210, 47-57.  
7 <https://doi.org/10.1016/j.cis.2013.10.018>.

8 Olofsson, U., Sundh, J., Bik, U., et al., 2015. The influence of snow on the tread  
9 braking performance of a train: A pin-on-disc simulation performed in a climate  
10 chamber. *Proc. Inst. Mech. Eng. Part F-J. Rail Rapid Transit.* 230(6),1512-1530.  
11 <https://doi.org/10.1177/0954409715616425>.

12 Ozbay, S., Erbil, H. Y., 2016. Ice accretion by spraying supercooled droplets is not  
13 dependent on wettability and surface free energy of substrates. *Colloid Surf. A-  
14 Physicochem. Eng.* 504, 210-218. <https://doi.org/10.1016/j.colsurfa.2016.05.065>.

15 Rashid, T., Khawaja, H. A., Edvardsenm, K., 2016. Review of marine icing and anti-  
16 /de-icing systems. *J. Mar. Eng. Technol.* 15(2), 79-87.  
17 <https://doi.org/10.1080/20464177.2016.1216734>.

18 Ringdahl, S., Xiao, S. B., He, J. Y., et al., 2021. Machine learning based prediction of  
19 nanoscale ice adhesion on rough surface. *Coatings.* 11(33), ID 33.  
20 <https://doi.org/10.3390/coatings11010033>.

21 Sabatier, J., Lanusse, P., Feytout, B., et al., 2016. CRONE control based anti-  
22 icing/deicing system for wind turbine blades. *Control Eng. Practice.* 56, 200-209.

- 1 <https://doi.org/10.1016/j.conengprac.2016.07.011>.
- 2 Tong, W., Xiong, D. S., Wang, N., et al., 2019. Mechanically robust superhydrophobic  
3 coating for aeronautical composite against ice accretion and ice adhesion.  
4 Compos. Pt. B-Eng. 176, ID 107267.  
5 <https://doi.org/10.1016/j.compositesb.2019.107267>.
- 6 Villegas, M., Zhang, Y. X., Abu Jarad, N., et al., 2019. Liquid-infused surfaces: a  
7 review of theory, design, and applications. ACS Nano 13(8), 8517-8536.  
8 <https://doi.org/10.1021/acsnano.9b04129>.
- 9 Wang, Z. W., Li, Q., She, Z. X., et al., 2012. Low-cost and large-scale fabrication  
10 method for an environmentally-friendly superhydrophobic coating on  
11 magnesium alloy. J. Mater. Chem. 22(9), 4097-4105.  
12 <https://doi.org/10.1039/C2JM14475A>.
- 13 Wang, F. J., Shen, T. H., Li, C. Q., et al., 2014. Low temperature self-cleaning  
14 properties of superhydrophobic surfaces. Appl. Surf. Sci. 317, 1107-1112.  
15 <https://doi.org/10.1016/j.apsusc.2014.08.200>.
- 16 Wang, Z. J., 2017. Recent progress on ultrasonic de-icing technique used for wind  
17 power generation, high-voltage transmission line and aircraft. Energy Build./  
18 Energ Buildings. 140, 42-49. <https://doi.org/10.1016/j.enbuild.2017.01.072>.
- 19 Work, A., Lian, Y. S., 2018. A critical review of the measurement of ice adhesion to  
20 solid substrates. Prog. Aeosp. Sci. 98, 1-26.  
21 <https://doi.org/10.1016/j.paerosci.2018.03.001>.
- 22 Xu, Q., Li, Z. Y., Wang, J., et al., 2012. Characteristics of single droplet impact on

1 cold plate surfaces. Dry. Technol. 30(15), 1756-1762.  
2 <https://doi.org/10.1080/07373937.2012.708001>.

3 Xia, H. Y., Zhao, X., Wu, Y. C., et al., 2020. Preparation and performance of  
4 antifreeze adhesive materials for asphalt pavement. Constr. Build. Mater. 258, ID  
5 119554. <https://doi.org/10.1016/j.conbuildmat.2020.119554>.

6 Yan, Y. D., Luo, N. Z., Xiang, X. G., et al., 2014. Fabricating mechanism and  
7 preparation of anti-icing & icephobic coating. Prog. Chem. 26(1), 214-222.  
8 <https://doi.org/10.7536/PC130633>.

9 Zhang, P., Lv, F. Y., 2015. A review of the recent advances in superhydrophobic  
10 surfaces and the emerging energy-related applications. Energy 82, 1068-1087.  
11 <https://doi.org/10.1016/j.energy.2015.01.061>.

12 Zheng, S. L., Li, C., Fu, Q. T., et al., 2016. Development of stable superhydrophobic  
13 coatings on aluminum surface for corrosion-resistant, self-cleaning, and anti-  
14 icing applications. Mater. Des. 93, 261-270.  
15 <https://doi.org/10.1016/j.matdes.2015.12.155>.

16 Zheng, H. K., Chang, S. N., Zhao, Y. Y., 2017. Anti-icing & Icephobic mechanism and  
17 application of superhydrophobic/ultra slippery surface. Prog. Chem. 29(1), 102-  
18 118. <https://doi.org/10.7536/PC161015>.

19 Zhuo, Y. Z., Xiao, S. B., Amirfazli, A., et al., 2021. Zhang, Polysiloxane as icephobic  
20 materials-The past, present and the future. Chem. Eng. J. 405, ID 127088.  
21 <https://doi.org/10.1016/j.cej.2020.127088>.

22

**Declaration of interests**

The authors declare that they have no known competing financial interests or personal relationships that could have appeared to influence the work reported in this paper.

The authors declare the following financial interests/personal relationships which may be considered as potential competing interests: